Supporting Information

Enhancing Backbone Regularity of Sulfurized Polyacrylonitrile for Long-Life Li-SPAN Batteries

Jiayu Wang[§], Zhen Du[§], Guijie Lv, Xiangyang Zhao, Chengming Li[*], Xiaonong Chen[*], Yaqin Huang[*]

Beijing Key Laboratory of Electrochemical Process and Technology for Materials, Key Laboratory of Biomedical Materials of Natural Macromolecules, Ministry of Education, Beijing University of Chemical Technology, Beijing 100029, PR China

[§]Co-first authors

[*]Email: huangyq@mail.buct.edu.cn

chenxn@mail.buct.edu.cn

lichm@mail.buct.edu.cn

Table S1 Element content analysis results of the PAN materials

Samples	Mass ratio (wt%)			Atom ratio		
	C	N	H	C	N	H
PAN	65.72	25.51	5.30	3.0	1.0	2.9
air160-PAN	67.40	26.29	5.34	3.0	1.0	3.1
air180-PAN	66.64	25.97	5.56	3.0	1.0	3.0
air200-PAN	66.08	25.55	5.30	3.0	1.0	2.9
air220-PAN	62.62	23.73	3.91	3.0	1.0	2.2
air240-PAN	62.55	22.54	3.18	3.0	0.9	1.8

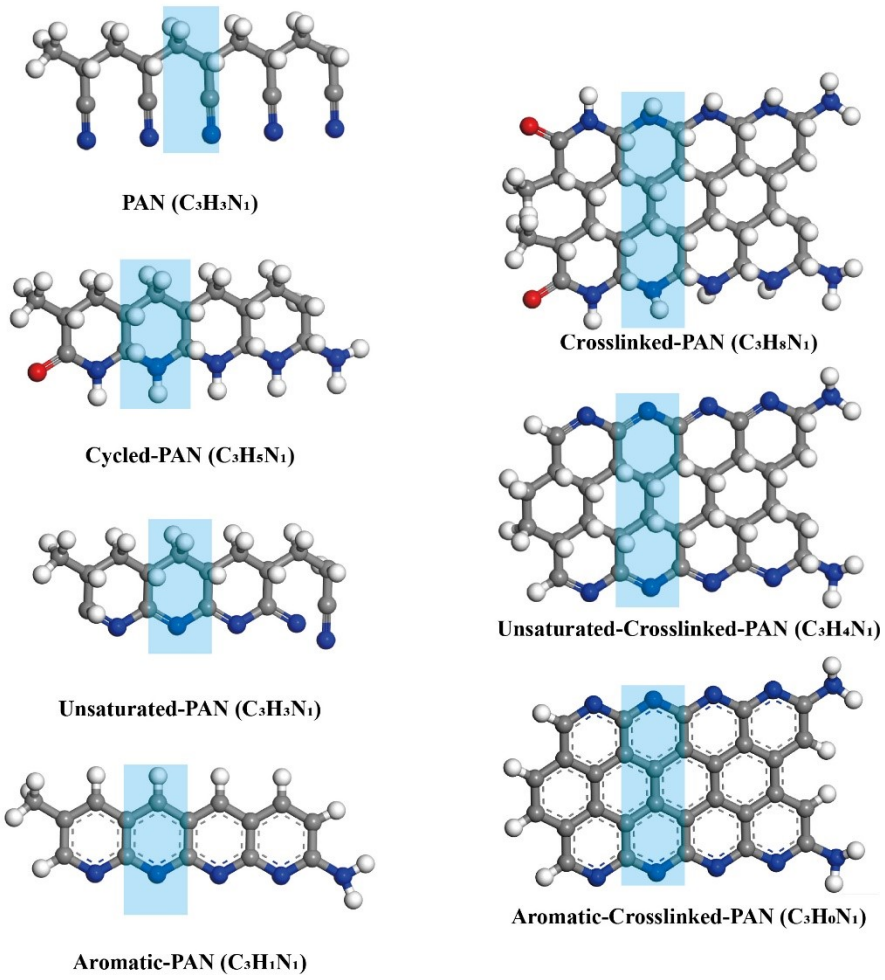

Figure S1 Molecular structures and the corresponding structural units that may exist in the pre-cyclization reaction.

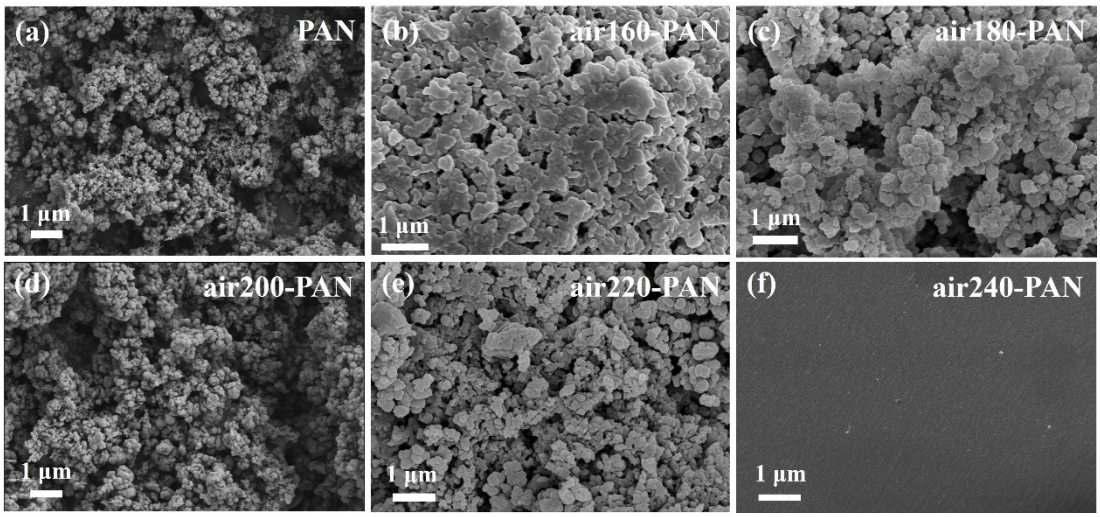

Figure S2 Low resolution SEM images of the oxidized polyacrylonitrile materials.

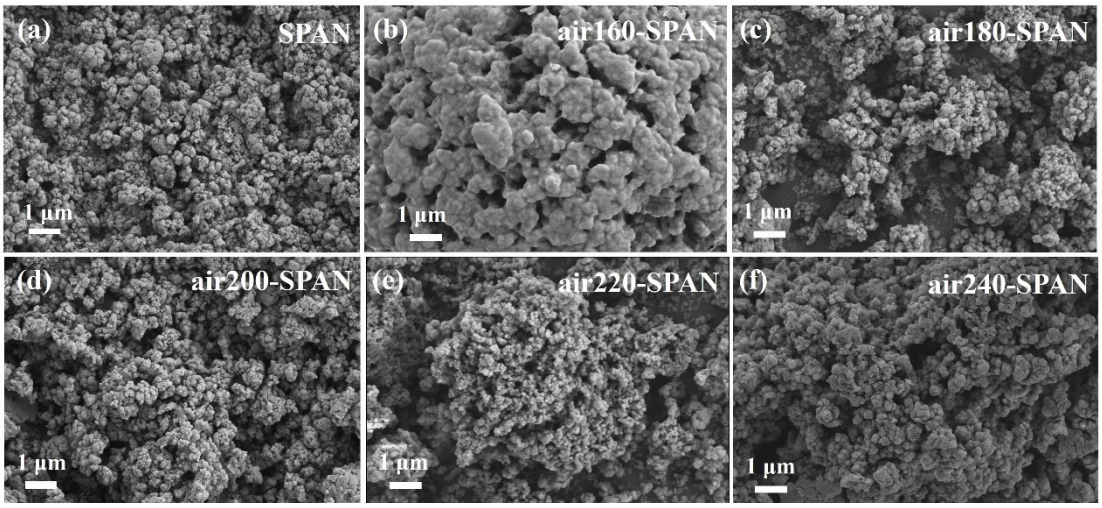

Figure S3 Low resolution SEM images of the sulfurized polyacrylonitrile materials.

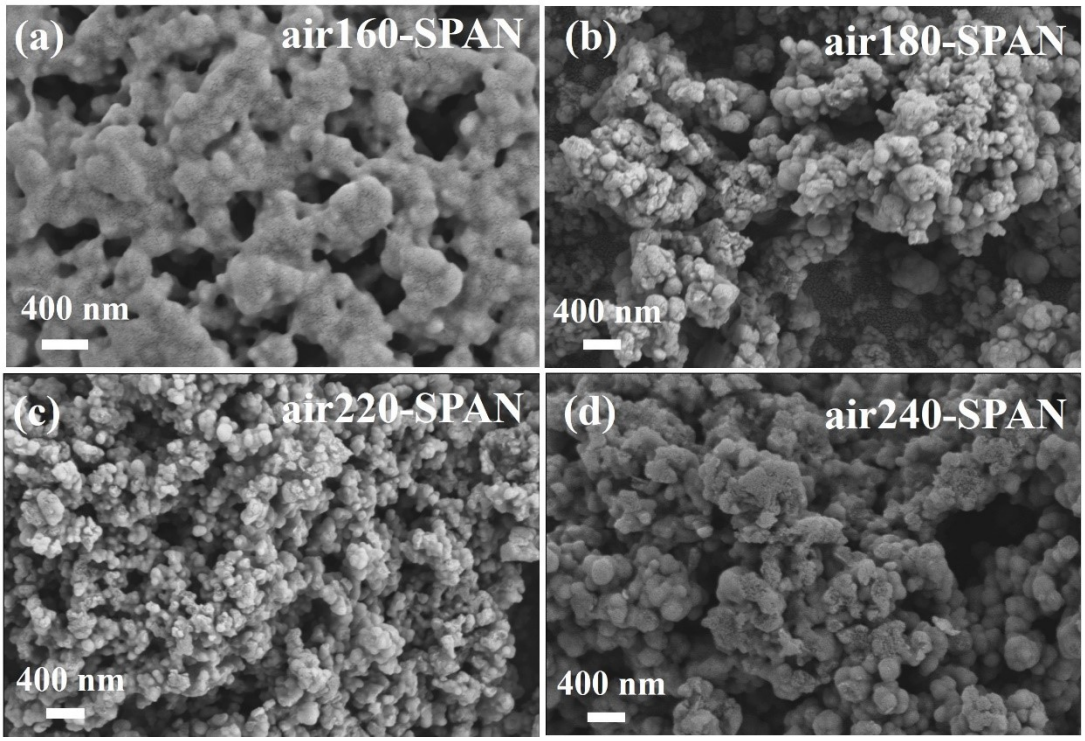

Figure S4 High resolution SEM images of the sulfurized polyacrylonitrile materials.

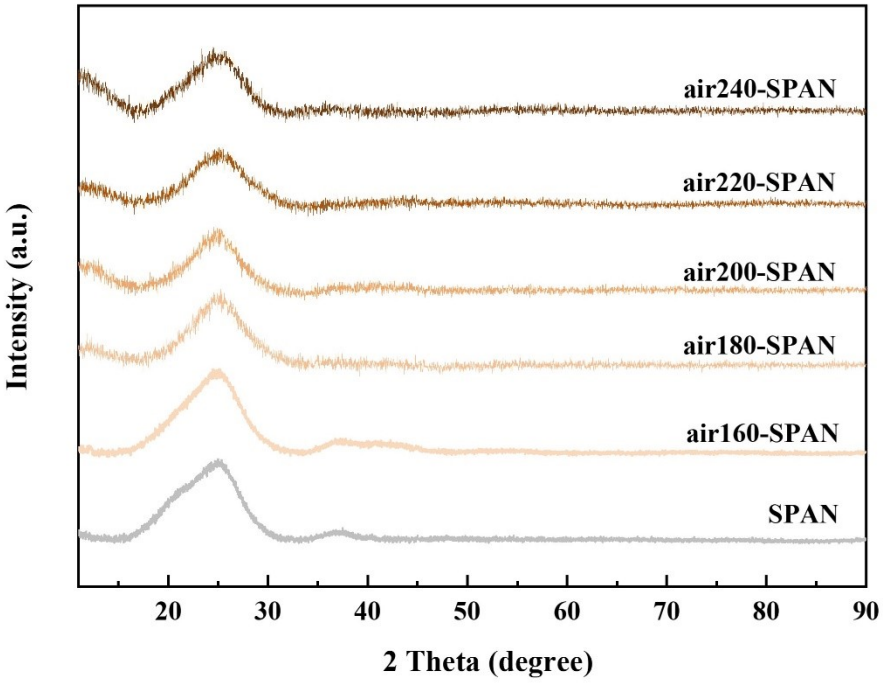

Figure S5 XRD patterns of the sulfurized polyacrylonitrile materials.

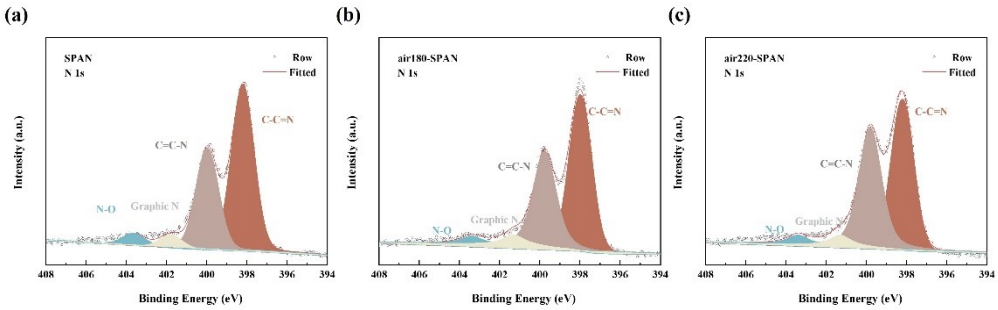

Figure S6 N 1s XPS spectra of (a) SPAN, (b) air180-SPAN and (c) air220-SPAN.

Table S2 Relative content of different nitrogen groups

Sample	N-O (%)	Graphic N (%)	C=C-N (%)	C-C=N (%)
SPAN	4	5	40	51
air160-SPAN	4	7	38	51
air180-SPAN	4	6	34	56
air200-SPAN	4	4	34	58
air220-SPAN	4	5	39	52
air240-SPAN	3	6	38	53

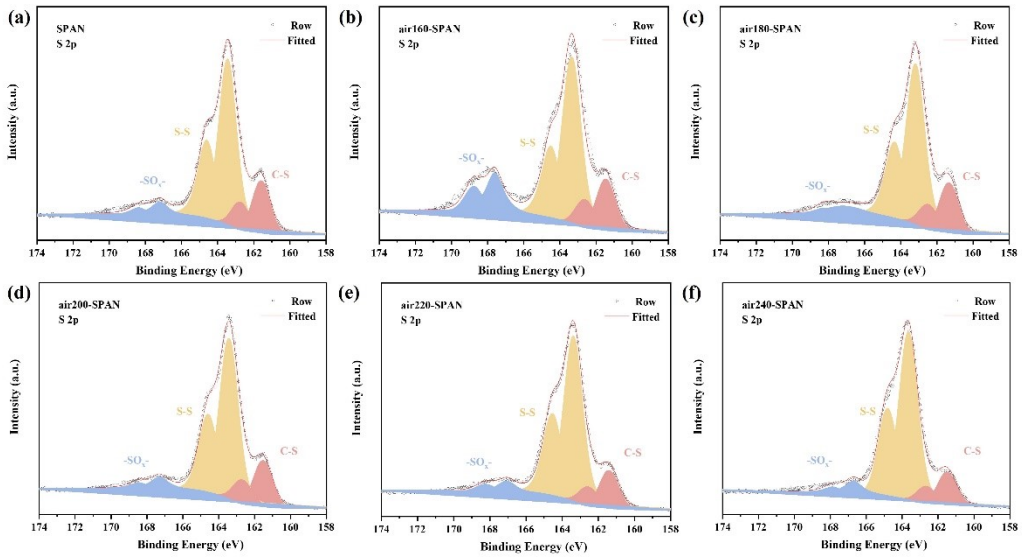

Figure S7 S 2p XPS spectra of the sulfurized polyacrylonitrile materials.

Table S3 Element content analysis results of the PAN materials

Samples	Mass ratio (wt%)			
	C	N	H	S
SPAN	38.04	13.41	0.58	43.81
air160-SPAN	38.51	14.31	0.40	43.45
air180-SPAN	38.55	13.85	0.38	43.51
air200-SPAN	39.22	14.12	0.35	43.64
air220-SPAN	41.94	15.34	0.65	36.10
air240-SPAN	52.94	18.86	1.57	18.77

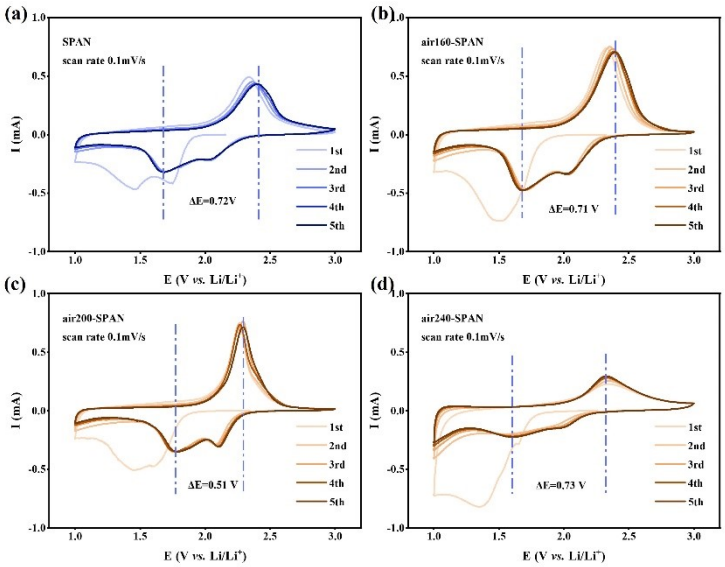

Figure S8 CV curves of the sulfurized polyacrylonitrile cathodes at a sweep rate of 0.1 mV s^{-1}.

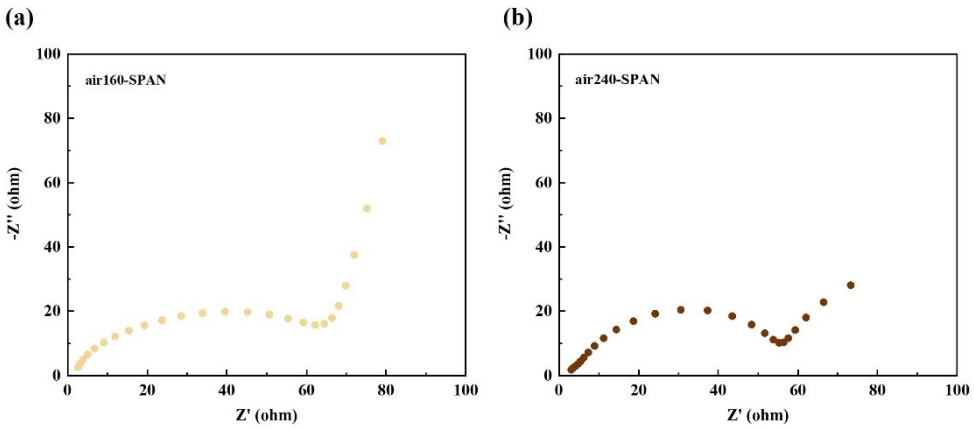

Figure S9 EIS Nyquist plots of the sulfurized polyacrylonitrile cathodes.

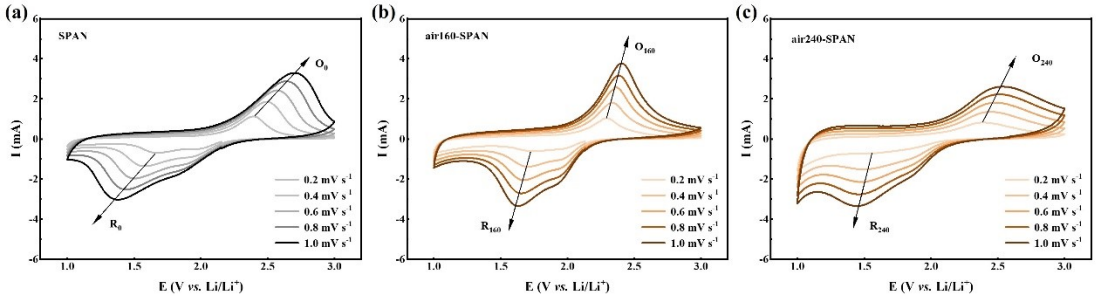

Figure S10 CV curves of the sulfurized polyacrylonitrile cathodes at various scanning rates.

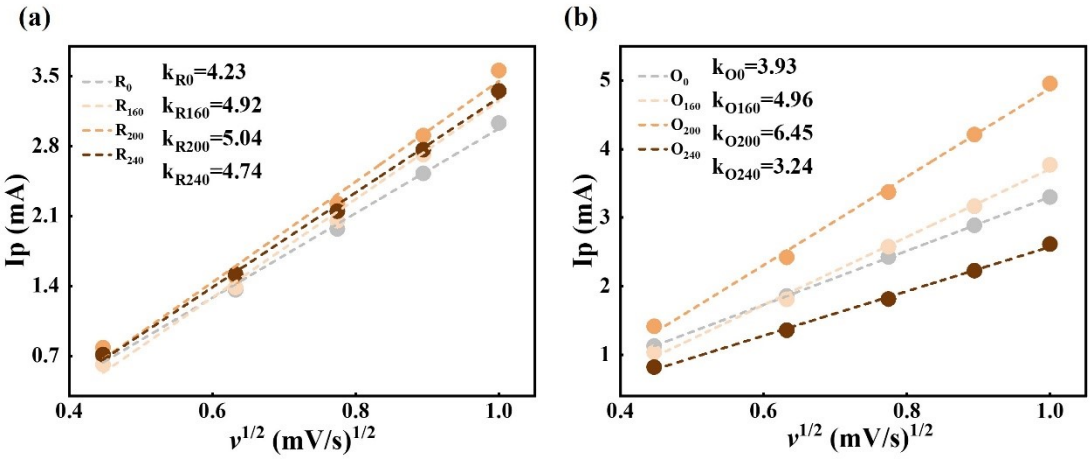

Figure S11 The linear fit profiles obtained from (e) reduction peaks and (f) oxidation peaks in cyclic voltammogram tests with various scanning rates.

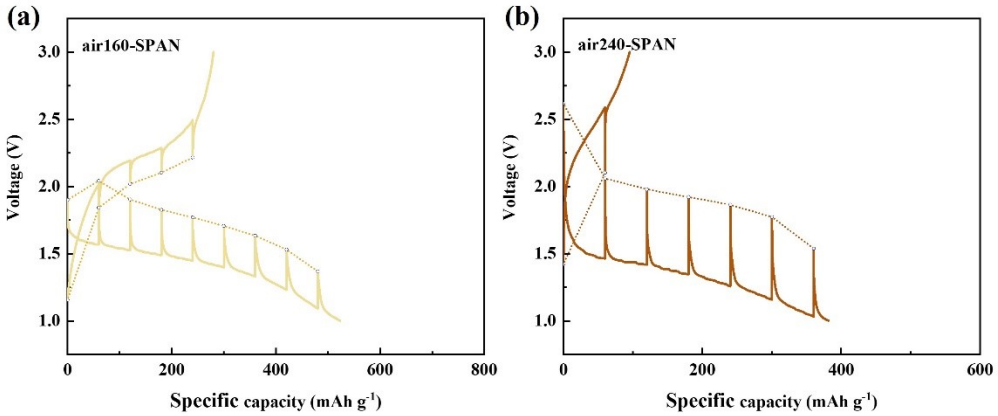

Figure S12 GITT potential profiles of the sulfurized polyacrylonitrile cathodes.

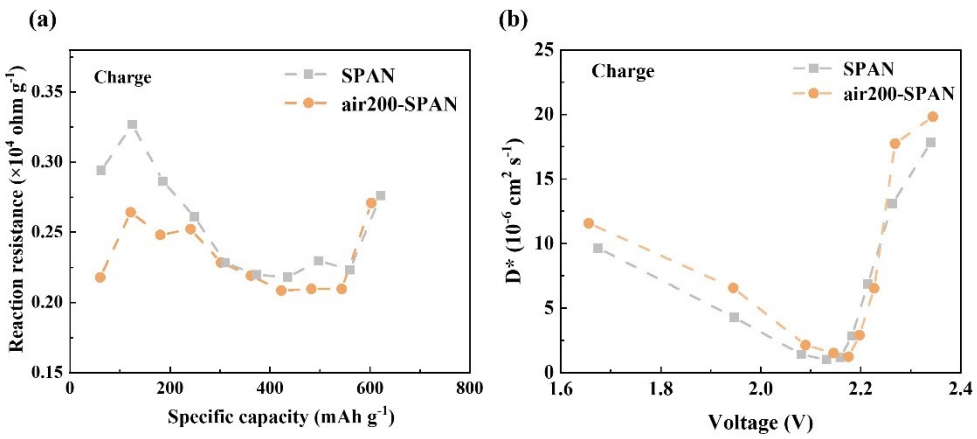

Figure S13 (a) Reaction resistance comparison of SPAN and air200-FSPAN during charge process. (b) Apparent diffusion coefficients calculated from the GITT potential profiles of SPAN and air200-SPAN for charge.

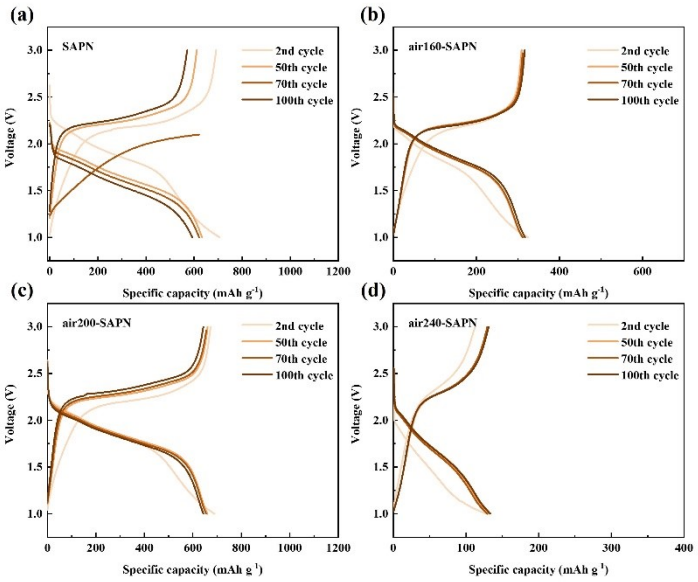

Figure S14 The charge and discharge profiles of the sulfurized polyacrylonitrile cathodes at 0.2 C.

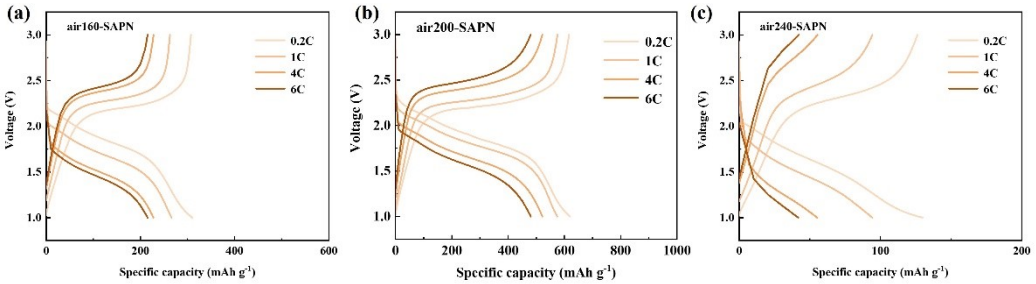

Figure S15 The charge and discharge profiles of the sulfurized polyacrylonitrile cathodes at different density.

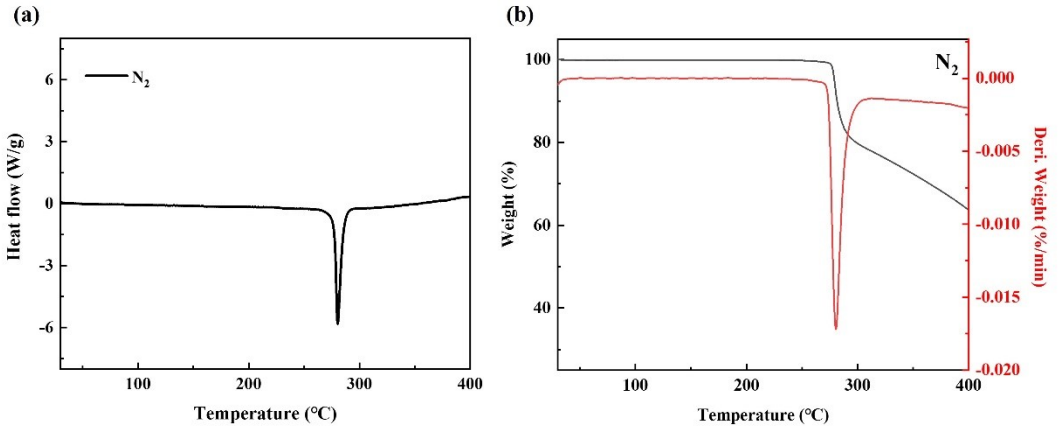

Figure S16 (a) DSC and (b) TG curves of PAN in nitrogen atmosphere.

Text S1: The DSC and TG tests of PAN were conducted under a nitrogen atmosphere (Figure S16). A sharp exothermic peak was observed at 280 ℃, accompanied by significant weight loss. Therefore, 280 ℃ was designed as the pre-cyclization reaction temperature under a nitrogen atmosphere. The PAN powder was placed in a quartz tube for pre-cyclization at 280 ℃ for 2 hours with a heating rate of 2 ℃ min^{-1}, and the obtained pre-cyclized PAN was noted as $N_2$280-PAN. The vulcanization process was the same as air*-SPAN, and the final product was denoted as $N_2$280-SPAN.

Table S4 Element content analysis results of the PAN materials

Samples	Mass ratio (wt%)				Atom ratio		
	C	N	H	S	C	N	H
$N_2$280-PAN	65.72	25.51	5.30	/	3.0	0.9	3.2
$N_2$280-SPAN	41.35	13.75	0.39	44.51	/	/	/

Text S2: The atom ratio of $N_2$280-PAN was normalized the same as Table S1. The atomic ratio of N (<1) and H (>3) indicates the reduction of backbone structure regularity, as well as the occurrence of dehydrogenation and cyclization.

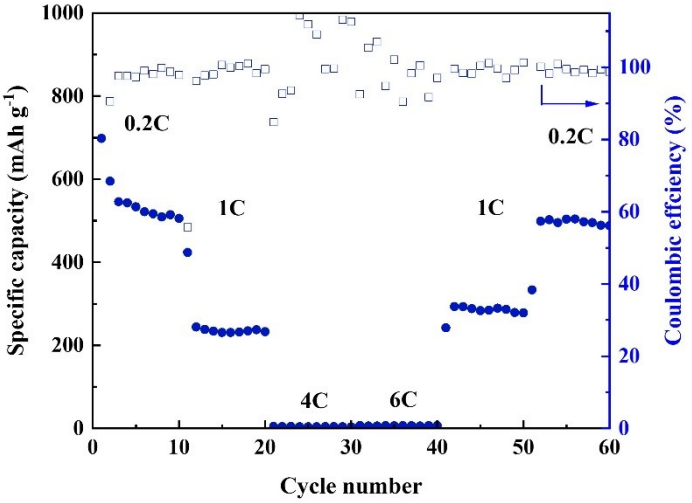

Figure S17 Rate performance of $N_2$280-SPAN.

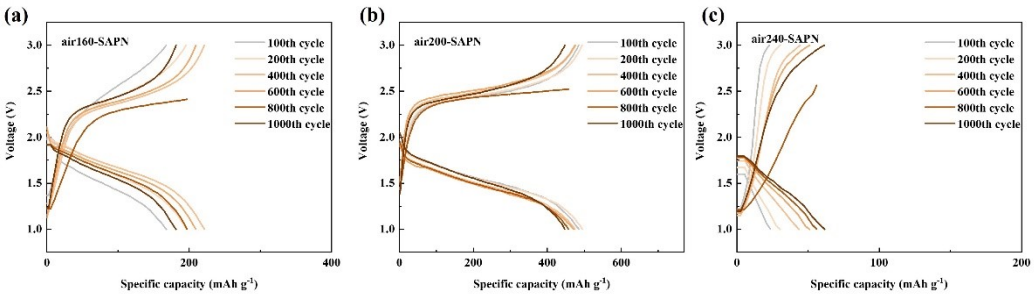

Figure S18 The charge and discharge profiles of the sulfurized polyacrylonitrile cathodes 3 C current density.

Table S5 Electrochemical performance of fibrous sulfurized polyacrylonitrile cathodes in lithium batteries

Cathode	Active material loading (mg cm^{-2})	Sulfur content (%)	Current density (A g_{SPAN}^{-1})	Cycles	Specific capacity (mAh g^{-1} based on SPAN)	Fading rate (%)	Ref.
SPAN/RGO	1.5	20.64	0.17	1000	123	/	[1]
$CoSe_2$-10@SPAN	1.67	47.1	0.47	500	317	0.058	[2]
SPAN-L	/	46.19	0.25	250	464	/	[3]
SPANM-HMTA	1.0	28.96	0.24	500	212	/	[4]
SPAN/CNT	2.0	37.60	0.38	400	440	/	[5]
FeMn@GN-SPAN	3.0	33.20	0.17	500	280	0.025	[6]
porous PAN/S	/	48	1.6	500	381	0.10	[7]
$Se_{0.03}$SPAN/CNT-3	5.2	51.97	0.87	800	323	0.021	[8]
SPANPPy-1%	1.5	43.3	0.74	500	368	/	[9]
S@PAN/S_7Se	5.0	68	1.36	500	440	0.047	[10]
SPPy320V	1.0	39.45	1.3	700	268	0.022	[11]
air200-SPAN	1.0	43.64	1.8	1400	427	0.01	This work

*The current density is calculated based on SPAN.

Reference

[1] Lu J, Zhang Y, Huang J, Jiang H, Liang B, Wang B, He D, Chen H. A Free-Standing Sulfide Polyacrylonitrile/Reduced Graphene Oxide Film Cathode with Nacre-Like Architecture for High-Performance Lithium-Sulfur Batteries[J]. Journal of Power Sources,2025, 629: 235916.

[2] Xu Z-Q, Zou R, Liu W-W, Liu G-L, Cui Y-S, Lei Y-X, Zheng Y-W, Niu W-J, Wu Y-Z, Gu B-N, Liu M-J, Ran F, Chueh Y-L. Design of Atomic Cobalt Selenide-Doped Sulfurized Polyacrylonitrile Cathode with Enhanced Electrochemical Kinetics for High Performance Lithium-Span Batteries[J]. Chemical Engineering Journal,2023, 471: 144581.

[3] Shi Z, Wang Y, Liu M, Ma J, Yue H, Hu Z, Yang S-T, Yin Y. Synthesis of Highly Cyclized Polyacrylonitrile Via Liquid-Phase Cyclization for Advanced Cathode Materials[J]. ACS Sustainable Chemistry & Engineering,2024, 12(49): 17806-17816.

[4] Hu X, Jiang H, Hou Q, Yu M, Jiang X, He G, Li X. Scalable Span Membrane Cathode with High Conductivity and Hierarchically Porous Framework for Enhanced Ion Transfer and Cycling Stability in Li–S Batteries[J]. ACS Materials Letters,2023, 5(8): 2047-2057.

[5] Huilan Li WX, Lina Wang, Tianxi Liu. Two Competing Reactions of Sulfurized Polyacrylonitrile Produce High-Performance Lithium-Sulfur Batteries[J]. ACS Appl Mater Interfaces,2021, 13(21): 25002-25009.

[6] Xiaomin Yuan BZ, Jinkui Feng, Chengguo Wang, Xun Cai, Rongman Qin. Feasible Catalytic-Insoluble Strategy Enabled by Sulfurized Polyacrylonitrile with in Situ Built Electrocatalysts for Ultrastable Lithium-Sulfur Batteries[J]. ACS Appl Mater Interfaces,2021, 13(43): 50936-50947.

[7] Wang K, Ju S, Gao Q, Xia G, Wang G, Yan H, Dong L, Yang Z, Yu X. Porous Sulfurized Poly(Acrylonitrile) Nanofiber as a Long-Life and High-Capacity Cathode for Lithium–Sulfur Batteries[J]. Journal of Alloys and Compounds,2021, 860.

[8] He R, Li Y, Wei S, Liu H, Zhang S, Han N, Liu H, Wang X, Zhang X. Construction of High-Performance Sulfurized Poly(Acrylonitrile) Cathodes for Lithium-Sulfur Batteries Via Catalytic and Conductive Regulation[J]. Journal of Alloys and Compounds,2022, 919.

[9] Yi Y, Hai F, Guo J, Gao X, Chen W, Tian X, Tang W, Hua W, Li M. Electrochemical Enhancement of Lithium-Ion Diffusion in Polypyrrole-Modified Sulfurized Polyacrylonitrile Nanotubes for Solid-to-Solid Free-Standing Lithium–Sulfur Cathodes[J]. Small,2023, 19(48): 2303781.

[10] He B, Rao Z, Cheng Z, Liu D, He D, Chen J, Miao Z, Yuan L, Li Z, Huang Y. Rationally Design a Sulfur Cathode with Solid-Phase Conversion Mechanism for High Cycle-Stable Li–S Batteries[J]. Advanced Energy Materials,2021, 11(14): 2003690.

[11] Yi Y, Hai F, Tian X, Wu Z, Zheng S, Guo J, Chen W, Hua W, Qu L, Li M. A Novel Sulfurized Polypyrrole Composite for High-Performance Lithium-Sulfur Batteries Based on Solid-Phase Conversion[J]. Chemical Engineering Journal,2023, 466: 143303.